

MODELING WAVE DISTORTION PHENOMENA IN MEDIA WITH LOCALIZED DAMAGE

K. Van Den Abeele⁺, F. Schubert[#], V. Aleshin⁺ and F. Windels⁺

⁺ Katholieke Universiteit Leuven Campus Kortrijk, Interdisciplinary Research Center, Kortrijk, Belgium

[#] Fraunhofer Institute for Nondestructive Testing, Branch Lab EADQ, Dresden, Germany

koen.vandenabeele@kula.ac.be

Abstract

A multiscale approach is proposed to predict the macroscopic amplitude dependent (i.e. nonlinear) behavior of the resonant mode response of a micro-inhomogeneous medium. To this extent, we assume that the mechanics of micro-inhomogeneities can be modeled by a two-step nonlinear hysteretic stress-strain relation at the microscopic level. At an intermediate scale (the mesoscopic scale) we calculate the equation of state using the well known Preisach-Mayergoyz (PM-space) model. Finally, upscaling to the macroscopic level is achieved by establishing a staggered grid formalism in space and time. Localized microdamage features in an intact medium are modeled by conceiving finite zones with pronounced hysteretic stress-strain relations within a “linear” surrounding. The simulations show a significant influence of the amplitude dependent resonance behavior on the location (edge versus center of a bar), the extend (width of the zone) and the degree (density of hysteretic units) of damage. Simple examples are given that illustrate the effects of thresholding and saturation of nonlinearity.

Introduction

One dimensional wave propagation and wave resonance in media with homogeneous distributions of elementary nonlinear and hysteretic units (interface contacts, cracks, weakened adhesion, etc) have been extensively described in the past by several groups [1-5]. When dealing with problems of wave propagation in media with non-uniform distributions of material properties, it becomes unavoidable to develop and apply appropriate numerical procedures. This has been performed successfully for the case of non-uniform linear material properties distributions [6-8] and is nowadays available in several commercial software packages. In the case of (hysteretic) nonlinear material properties, distributed non-uniformly over a sample, there has been no reports to our knowledge that deal with wave propagation or resonance. However, this topic is of particular interest in the field of non-destructive testing, since it is critical to the understanding of the macroscopic nonlinear behavior of materials with localized damage. Besides, an appropriate simulation model can be used as the basis for establishing sensitive nonlinear imaging techniques.

Numerical Multiscale Nonlinear Model

The modeling of damage features in a material requires the introduction of locally nonlinear and non-unique equations of state. In order to account for these local properties, we introduce the multiscale concept that is illustrated in Figure 1. An object (macroscopic level M) is divided into a number of mesoscopic (level m) material cells. Each mesoscopic cell is thought of as being composed of a statistical ensemble of microscopic units (level μ) with varying properties defining their mechanical stress-strain relation. These microscopic units represent the grains and the complex contacts between individual grains. Length scales associated to each level are of the order 0.1-1 m for the macroscopic level, 1-10 mm for the mesoscopic level and 1-100 μm for the microscopic scale.

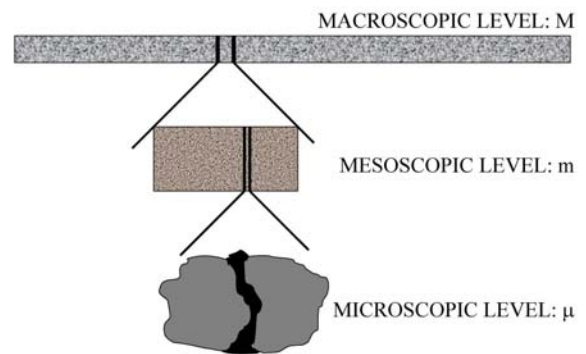


Figure 1: The Multiscale concept

At the *microscale level*, the strain response of the individual units is modeled through a combination of a classical nonlinear state relation, and a non-classical addition because of hysteresis effects (i.e. non-uniqueness in the stress-strain behavior): $\varepsilon = \varepsilon_C + \varepsilon_H$. The classical strain component ε_C can be linked to the traditional nonlinear powerlaw relation between stress (σ) and strain (ε), as being used for describing nonlinearity in liquids and single crystals. However in this paper we focus on non-classical nonlinearity and therefore we assume that the classical contribution to the strain response reduces to the Hooke's law: $\varepsilon_C = \sigma/K$, with K the modulus. The hysteretic strain component, ε_H , arises from the following basic idea of crack opening and closure: For increasing stress, the strain contribution is zero for $\sigma < \sigma_c$ (“open” state), and γ for $\sigma > \sigma_c$ (“closed” state). For decreasing stress, the strain contribution equals γ for $\sigma > \sigma_0$ (“closed” state)

and zero for $\sigma < \sigma_o$ ("open" state). Here, $\sigma_c > \sigma_o$. For simplicity we assume that only the parameters σ_o and σ_c can vary from microscopic unit to microscopic unit. When looking at all microscopic units within a material cell, we assume that all other parameters remain constant, i.e., K and γ are "effective" material cell constants which are defined at the *mesoscopic level*. The collection of all units within a material cell can be represented in a stress-stress space according to their values. σ_c and σ_o , commonly termed the "PM-space", and mathematically represented by its density distribution $\rho_{PM}(\sigma_c, \sigma_o)$ [9-11]. In this way, the two effective material constants, K and γ , together with the particular PM-space density form a unique characteristic of the material cell. This ID obviously may differ from cell to cell. For instance, the PM-space distribution of a linear material cell is empty (or equivalently: $\gamma=0$), the PM-space of a damaged cell has a non-zero value for γ and a non-zero density. Some simple distributions of PM-spaces are shown in figure 2, in which we depicted a uniform PM-space, an offset-ed PM space, a finite banded PM-space and a localized PM-space. In each subfigure we assume that the gray areas correspond to uniform but non-zero densities.

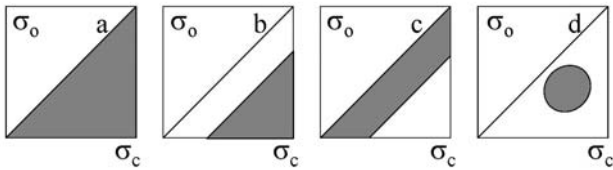


Figure 2: Mesoscopic level PM-space distributions

The mesoscopic stress-strain relation of each material cell can be calculated from the incremental form of the relationship between the stress increase/decrease from σ_1 to σ_2 and its corresponding strain response [12]:

$$\Delta \varepsilon = \Delta \varepsilon_C + \Delta \varepsilon_H = \frac{\sigma_2 - \sigma_1}{K} + \gamma (f_c(\sigma_2) - f_c(\sigma_1))$$

with $f_c(\sigma_i)$ for $i=1,2$ the fraction of microscopic units within the material cell which are in a "closed" state at the stress σ_i . It is important to realize that this function is highly dependent on the stress history, σ_{his} .

The up-scaling from mesoscopic level to *macroscopic level* is based on the formalism of EFIT (Elastodynamic Finite Integration Technique), which was originally developed by Fellingner et al.[6-8]. The formalism uses a velocity-stress discretisation of the equation of motion and of the rate formulation of the above specified equation of state. In 1D, the discretised equations of the EFIT code are similar to those of a Finite Difference Time Domain (FDTD)

scheme on a staggered temporal and spatial grid. Particular care must be taken in the handling of the discretised rate formulation of the equation of state, since it involves the derivative of the function $f_c(\sigma)$ with respect to σ , which represents the change in the fraction of the PM-space area occupied by closed units for a infinitesimal change of σ . This quantity is highly dependent on the previous history of the stress.

Simulations

In the simulations, we assume a 1D cylindrical bar of a fictitious material with modulus $K=10$ GPa, material density $\rho=2600$ kg/m³, inverse attenuation (or quality factor) $Q=80$, and length $L=0.25$ m. To perform the simulations we assume an initial condition of rest and a continuous sinusoidal forcing $F \sin(2\pi ft)$ at the boundary ($x=0$). For each forcing amplitude (F) and excitation frequency (f), the numerical multiscale model calculates the distribution of stress and velocity over the bar at each step in time, and stores the Fourier components of the steady state velocity response at $x=L$ of the sample after $5Q$ cycles. The frequency is swept in discrete steps around the fundamental longitudinal resonance frequency of the cylindrical bar. This allows us to analyze (fundamental and harmonic) resonance curves at various driving force, and to determine the peak coordinates of the resonance line at each forcing level. The peak amplitude can be easily converted in the maximal strain response amplitude $\varepsilon_{1r}(F)$ for the given forcing F , the peak frequency is the resonance frequency $f_r(F)$ of the system at that forcing. From this analysis, we determine the relative changes in the resonance frequency (i.e. $(f_r(F_0) - f_r(F)) / f_r(F_0) = \Delta f_r(F) / f_r(F_0)$ with F_0 an extremely small value yielding the linear resonance frequency) as a function of the peak strain amplitude $\varepsilon_{1r}(F)$ measured at the same forcing. The resultant dependence relation quantifies the effect of hysteresis and nonlinearity on the modulus. In addition we also determine the strain amplitude of the third harmonic $\varepsilon_{3r}(F)$ at the resonance frequency $f_r(F)$ for the different forcing values (even harmonics are not created in a purely hysteretic medium), and analyze these values against the peak strain amplitude $\varepsilon_{1r}(F)$ of the fundamental component in the response. Doing so, we quantify the effect of hysteresis and nonlinearity on the generation of harmonics.

At first, we have checked and confirmed the usual dependencies which are expected in the case of identical material cells (mesoscopic level), with uniform PM-spaces (i.e. uniform distributions of microscopic units over the σ_o - σ_c space): 1) Both the resonance frequency and the quality factor diminish linearly with the fundamental strain response amplitude (i.e. $\Delta f_r(F) / f_r(F_0) = \alpha_f \varepsilon_{1r}(F)$, and $\Delta Q(F) / Q(F_0) = \alpha_Q \varepsilon_{1r}(F)$); 2) The third and all higher odd

harmonics in the strain response depend quadratically on the fundamental strain response amplitude (i.e. $\epsilon_{3r}(F) = \alpha_3 (\epsilon_{1r}(F))^2$, etc.); 3) the proportionality coefficients in all of these relations are increasing linearly with the value of the hysteretic strength γ .

To model the effects of local damage features in a material, we have introduced finite zones with pronounced hysteretic stress-strain relations within a "linear" surrounding. In the following, we illustrate the influence of the localization, the extend and the nature of damage by varying the position of the hysteretic zone, the width of the zone and the PM-space distribution of one or more mesoscopic cells.

We first investigate the nonlinear parameter sensitivity variation with the position x_d of a damage zone of width $L/40$. Inside the damaged zone, we assume a uniform PM-space distribution of hysteretic units. All other material cells are considered to be purely linear. The numerical results and their subsequent analysis showed that the above mentioned dependence relation for resonant frequency shift and third harmonic are still maintained. At each position x_d of the damage, we determined α_f and α_3 , and the results are shown in Figure 3. Obviously the dependence of the resonance frequency shift on the response amplitude, and the quadratic dependence of the third harmonic are both highly influenced by the position of the hysteretic nonlinear material cell within the bar. Since the strain of the first longitudinal mode is largest in the center of the bar and zero at the edges, it is no surprise that the sensitivity will be largest when damage is situated in the center of the sample, and that there is almost no sensitivity to damage at the edges. An analytical model, developed by Windels and Van Den Abeele [13] and applied to hysteretic stress-strain relations, confirms the position dependent sensitivity and explicitly predicts a $(\sin(\pi x_d/L))^3$ behavior (full line in the top plot of Figure 3). The variation of the third harmonic proportionality coefficient is somewhat more complicated and shows two zones of strongly reduced sensitivity. This is due to the highly structured shape of the strain pattern of the third fundamental resonance, which has two positions of zero strain. Here, the analytical model of Windels and Van Den Abeele predicts a $(\sin(\pi x_d/L))^2 \sin(3\pi x_d/L)$ behavior. This is illustrated by the full line in the bottom plot of Figure 3. Finally, it is important to note that this analysis predicts conditions for which there can be a resonance frequency shift without the observation of a third harmonic, e.g. when the damage is located at $x_d=L/3=0.083m$.

The influence of the width of the damage zone on the proportionality coefficients α_f and α_3 is illustrated in Figure 4. Here, we have considered a finite damage zone of variable width, centered along the bar. Again, we assume a uniform distribution of hysteretic

elements in the PM-spaces of the material cells that contain the damage. The width is increased from $L/20$ (2 material cells containing damage) to L (all material cells containing damage). The fact that damage which is located at the bar edges does not influence the modulus reduction is clearly confirmed by the observed saturation of the coefficient α_f . However, the

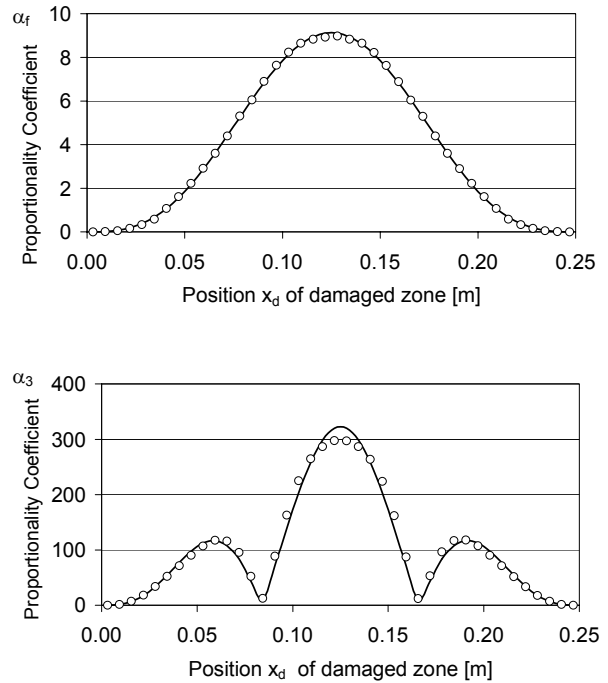


Figure 3: Nonlinearity sensitivity to damage position (Numerical model (open circles) and analytical prediction (full line))

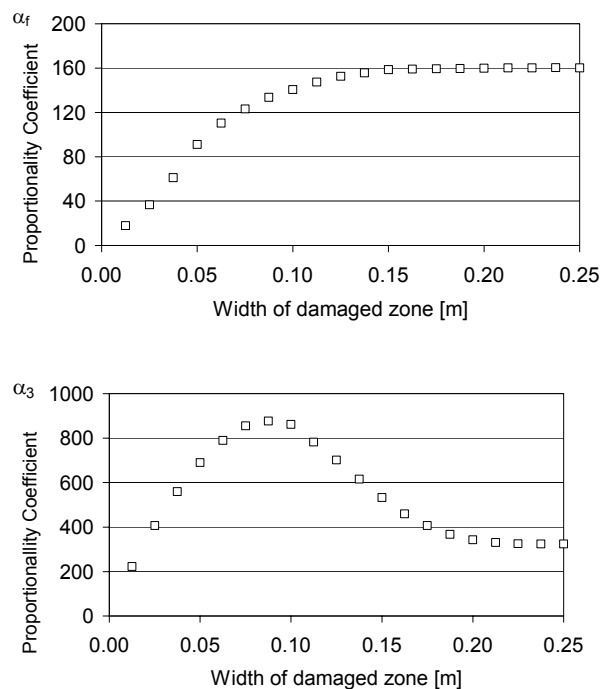


Figure 4: Nonlinearity sensitivity to damage width

extension of the damaged zone towards the bar edges reduces the rate at which the third harmonic increases with excitation. Indeed, once the damaged zone is larger than $L/3$ (and centered in the bar) the third harmonic generation diminishes. Apparently the nonlinearity is constructively accumulated for $W < L/3$, and interferes destructively (because of the anti-phase lobes of the third order resonance mode) when $W > L/3$.

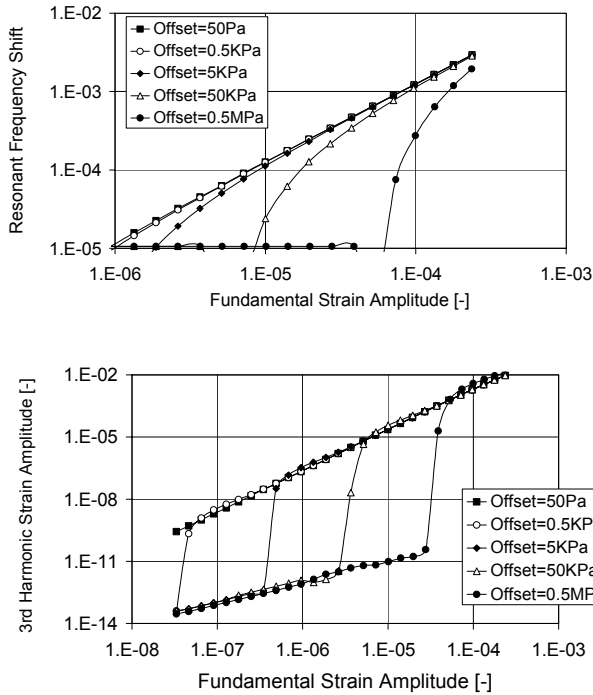


Figure 5: Thresholding effects in nonlinear behavior.

The degree of damage can be varied by playing with the parameter γ . However, it is also possible to investigate the influence of the microstructural units within the PM-space of each mesoscopic cell. These units can be uniformly distributed over the complete PM-space (figure 2a) or can be located at specific areas, for instance, only away from the diagonal in the σ_o - σ_c space or only near the diagonal, or in a restricted area (see Figure 2b-d). Figure 5 illustrates the influence of an increasing off-set in the distribution of the PM-space elements for all material cells in the macroscopic object. The resonance frequency shift versus strain amplitude and the third harmonic strains clearly show a threshold behavior at strains which closely correspond to the a priori assumed stress off-sets (remember that $K=10$ GPa). On the other hand, it is not hard to understand that a finite band of uniformly distributed microscopic units adjacent to the diagonal will introduce a saturation effect of the nonlinear response, as is illustrated in Figure 6 for decreasing PM-space widths. Finally, a localized distribution of elements in the PM-space can introduce as well thresholding effects as saturation

effects, which can disturb the traditional expectations of resonant frequency shifts to a large extent.

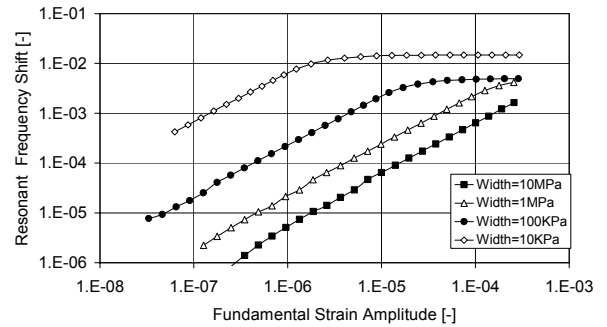


Figure 6: Saturation of nonlinearity

Acknowledgements

The authors acknowledge the support of this work by the ESF-PESC NATEMIS program, by the Foundation for Scientific Research of Flanders and by the European FP5 program DIAS (EVK4-2001-00141).

References

- [1] K. Van Den Abeele, R.A. Guyer, K. R. McCall, P. A. Johnson, *J. Acoust. Soc. Am.* 101, 1885, 1997
- [2] R.A. Guyer, K. R. McCall, K. Van Den Abeele, *Geophys. Res. Lett.* 25, 1585, 1998.
- [3] M. Scalerandi, P.P. Delsanto, V. Agostini, K. Van Den Abeele, P.A. Johnson, *J. Acoust. Soc. Am.* 113, 3049, 2003.
- [4] V. Gusev, *J. Acoust. Soc. Am.* 107, 3047, 2000.
- [5] V. Gusev and V. Aleshin, *J. Acoust. Soc. Am.* 112, 2666, 2002.
- [6] P. Fellingner, R. Marklein, K.J. Langenberg, and S. Klaholz, *Wave Motion* 21, 47, 1995.
- [7] F. Schubert and B. Koehler, in: *Nondestructive Characterization of Materials VIII*, Plenum, New York, 567, 1998.
- [8] F. Schubert and B. Koehler, *J. Comp. Acoust.* 9, 1543, 2001.
- [9] K.R. McCall and R.A. Guyer, *J. Geophys. Res.* 99, 23887, 1994.
- [10] K.R. McCall and R.A. Guyer, *Nonlinear Processes in Geophys.* 3, 89, 1996.
- [11] R.A. Guyer, K.R. McCall, G.N. Boitnott, L.B. Hilbert Jr., and T.J. Plona, *J. Geophys. Res.* 102, 5281, 1997.
- [12] J. Carmeliet and K. Van Den Abeele, *Geophys. Res. Lett.* 29(7), 1144, 2002.
- [13] F. Windels and K. Van Den Abeele, see proceedings WCU'03, Paris 2003.